

Few-Shot Traffic Prediction with Graph Networks using Locale as Relational Inductive Biases

Mingxi Li, Yihong Tang, Wei Ma[†], *Member, IEEE*

Abstract—Accurate short-term traffic prediction plays a pivotal role in various smart mobility operation and management systems. Currently, most of the state-of-the-art prediction models are based on graph neural networks (GNNs), and the required training samples are proportional to the size of the traffic network. In many cities, the available amount of traffic data is substantially below the minimum requirement due to the data collection expense. It is still an open question to develop traffic prediction models with a small size of training data on large-scale networks. We notice that the traffic states of a node for the near future only depend on the traffic states of its localized neighborhoods, which can be represented using the graph relational inductive biases. In view of this, this paper develops a graph network (GN)-based deep learning model LOCALEGN that depicts the traffic dynamics using localized data aggregating and updating functions, as well as the node-wise recurrent neural networks. LOCALEGN is a light-weighted model designed for training on few samples without over-fitting, and hence it can solve the problem of few-shot traffic prediction. The proposed model is examined on predicting both traffic speed and flow with six datasets, and the experimental results demonstrate that LOCALEGN outperforms existing state-of-the-art baseline models. It is also demonstrated that the learned knowledge from LOCALEGN can be transferred across cities. The research outcomes can help to develop light-weighted traffic prediction systems, especially for cities lacking in historically archived traffic data.

Index Terms—Traffic Prediction; Few-shot Learning; Graph Networks; Transfer Learning; Intelligent Transportation Systems

I. INTRODUCTION

SMART traffic operation and management systems rely on accurate and real-time network-wide traffic prediction [1, 2], and it is the essential input for various smart mobility applications such as personal map services [3], connected and autonomous vehicles [4], traffic signal control [5], and advanced traveler information system/advanced traffic management system (ATIS/ATMS). In many megacities like Los Angeles and New York, massive traffic data have been

M. Li is with the Department of Civil and Environmental Engineering, The Hong Kong Polytechnic University, Hong Kong SAR, China (E-mail: mingxi-chloe.li@connect.polyu.hk).

Y. Tang is with the Department of Computer Science and Technology, Beijing University of Posts and Telecommunications, Beijing, China (E-mail: tyh@bupt.edu.cn).

W. Ma is with the Department of Civil and Environmental Engineering, The Hong Kong Polytechnic University, Hong Kong SAR, China; The Hong Kong Polytechnic University Shenzhen Research Institute, Shenzhen, Guangdong, China; and Research Institute for Sustainable Urban Development, The Hong Kong Polytechnic University, Hong Kong SAR, China (E-mail: wei.w.ma@polyu.edu.hk).

[†]: Corresponding author.

Manuscript received: March 9, 2022.

collected and archived, which include vehicle speeds, traffic volumes, origin-destination (OD) matrices, etc., and these data are widely used to generate traffic predictions. Among different traffic prediction models, deep neural networks, especially the graph-based neural networks, such as graph convolutional networks (GCN) [6, 7], achieve state-of-the-art accuracy and have been widely deployed in various industry-level smart mobility applications. For example, Uber has been using deep learning for travel time prediction [8].

To further improve the prediction accuracy on large-scale transportation networks, the model complexity and number of trainable parameters of the newly developed traffic prediction models have increased drastically in recent years [9, 10]. Most of the existing models require the historically archived traffic data for a long time period, and we define the length of the time period as the data size [11]. In contrast, the size of the transportation network is referred to as the network size. In Figure 1, we present the relationship between the network size and data size with respect to the number of trainable parameters and prediction accuracy for existing traffic prediction models.

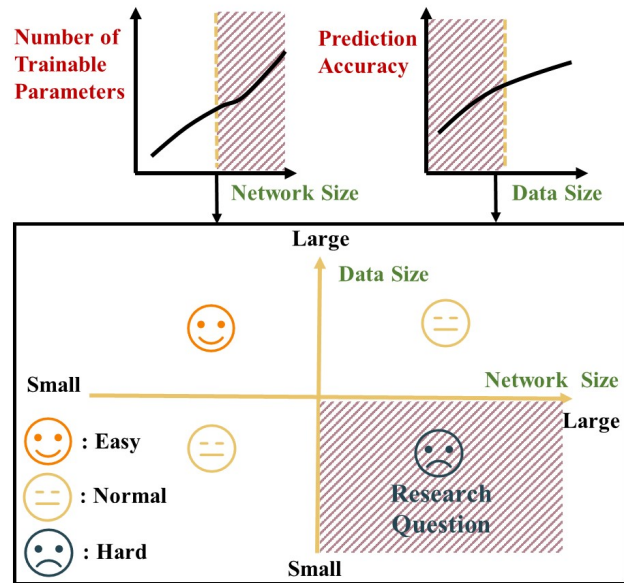


Fig. 1: Relationship of network and data size for current traffic prediction models.

In general, traffic prediction accuracy increases with respect to the data size, and the number of trainable parameters number increases with respect to the network size. When the network size becomes larger, more data (longer time period

of historical data) is required to prevent overfitting due to a large number of trainable parameters [12]. Overall, existing well-performed deep learning models require a large data size for training to ensure good performance on the large-scale networks. However, because of the high expenses in data collection and sensor maintenance [13], it is not practical to expect every city to archive a comprehensive and long-history dataset. As shown in Figure 1, how to develop traffic prediction models with a small data size on the large-scale networks is the key research question addressed in this paper.

We further motivate this study using a practical example. Hong Kong aims to transform itself into a smart city within the next decade, and the Smart City Blueprint for Hong Kong 2.0 was released in December 2020, which outlines the future smart city applications in Hong Kong [14]. The blueprint plans to “complete the installation of about 1,200 traffic detectors along major roads and all strategic roads to provide additional real-time traffic information” for Hong Kong’s smart mobility system. Consequently, Hong Kong’s Transport Department is gradually installing traffic sensors and releasing the data starting from the middle of 2021 [15]. As shown in Figure 2, the number of traffic sensors increases drastically in the recent year. The duration of the historical traffic data from the new sensors can be less than one month, making it impractical to train existing traffic prediction models. Similar situations also happen in many cities like Paris, Shenzhen, and Liverpool [16], as the concept of smart cities just steps into the deployment phase globally. Therefore, a network-wide traffic prediction model, which achieves the state-of-the-art performance with a small size traffic data, could enable the smooth transition and early deployment of smart mobility applications [17]. Hence this study has practical values for many cities.

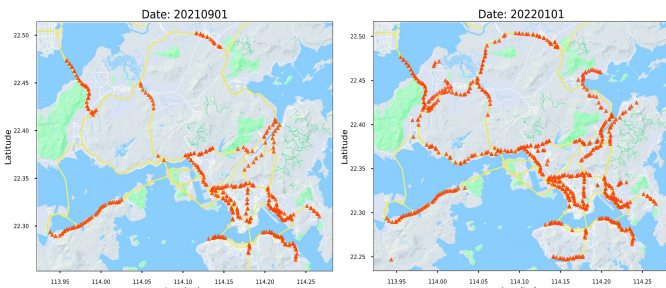


Fig. 2: Distribution of available detectors in Hong Kong in September 2021 (left) and January 2022 (right).

To this end, we define the task of few-shot traffic prediction, which aims to train on historical traffic data with a short history, and generate accurate short-term traffic prediction on the large-scale networks. This task is essentially challenging as the complicated prediction model on large-scale network is prone to overfit with limited data [18, 19]. To address this issue, we notice that the short-term traffic state on a certain node (target node) only depends on the traffic states of its localized neighbors. More specifically, as shown in Figure 3, the traffic state at time $\tau + 1$ is mainly affected by the traffic states of itself and its neighborhoods at time τ . It is straightforward to observe that the change of traffic state on a

node is attributed to the traffic (e.g., vehicle, flow) exchanges, then the nodes far away from the target node cannot exchange traffic directly with the target node, and hence the impact of those nodes are indirect and marginal. We define the concept **locale** of a target node as a collection of information on its neighboring nodes, and the information includes, but is not limited to traffic states (e.g., speed, flow, OD), static data (e.g., road type, speed limit), and auxiliary information (e.g., weather). Finally, it is safe to claim that the traffic state of the target node in the near future mainly depends on its current locale.

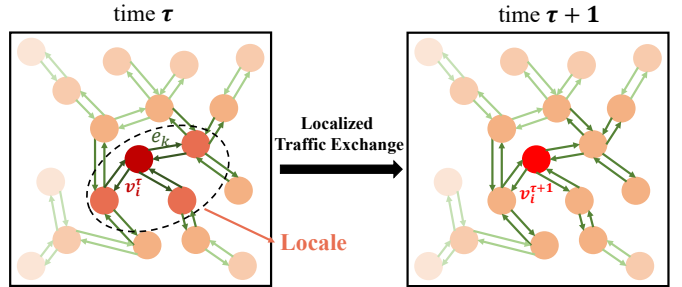


Fig. 3: Illustration of the concept of locale.

The locale of a node can be viewed as the relational inductive biases for the prediction model, which enforces the entity relations in a deep learning architecture. In our case, the connections between nodes allow the traffic exchanges, while no direct traffic exchanges are allowed if two nodes are not connected. Additionally, other static information such as location information and road properties affect the speed and frequency of those traffic exchanges. To make use of the relational inductive biases, we adopt the Graph Network (GN) to capture the dynamic and localized traffic states of a target node. The GN demonstrates great potential in modeling the relational inductive biases and has been widely used to depict the localized relationship among different entities [20]. It is also a generalized form of many existing graph-based network structures [21, 22]. In this paper, we extend the GN model to learn the *locally spatial* and temporal patterns of traffic states for generating predictions. Importantly, GN is applied to each node separately, and it can be applied to different nodes with various topologies. GN is also light-weighted with a small number of trainable parameters, making it easy to train given the limited training samples.

It is noteworthy that the similar concept of locale is widely adopted for the spatial approaches of the graph neural networks (GNN) defined in [6], and one of the representative examples is the message passing neural network (MPNN) [23]. However, current traffic prediction models overlook the properties of locale and rely on GNN to implicitly learn the locally spatial dependency of the traffic states, which also explains why the existing traffic prediction models generally require a large amount of data. To the best of our knowledge, among the commonly used traffic prediction models, DCRNN and WAVENET depict the diffusion process of traffic states, which share the most similar idea to locale [24, 25]. However, due to their complex model structures, the performance of both

models degrade drastically with a few data samples, which will later be shown in the numerical experiments. This observation also suggests a light-weighted structure for the few-shot traffic prediction task.

To summarize, the small data size and large network size present great challenges to existing traffic prediction models, and it is promising to utilize the localized traffic information and data (locale) to generate traffic predictions without modeling the entire network simultaneously. In view of this, this paper proposes Localized Temporal Graph Network (LOCALEGN) to model the *locally spatial* and temporal dependencies on graphs for predicting traffic states in the near future. This is the first time that GN is adopted and extended for traffic prediction tasks, and the choice of GN is attributed to its previous successful applications in predicting the physical systems, such as fluid dynamics and glassy systems [20]. LOCALEGN can learn from different nodes on the large network, and hence it can be declared as a light-weighted model to make accurate short-term predictions from few training samples. The contribution of this paper can be summarized as follows:

- We propose the few-shot traffic prediction task and highlight the importance of using localized information (locale) of each node to address the issue of lacking data in the proposed task.
- We develop a *locally spatial* and temporal graph architecture LOCALEGN for the few-shot traffic prediction task. The *locally spatial* pattern is modeled by the graph network with relational inductive biases, and the temporal pattern is depicted with a modified recurrent neural network.
- We conduct experiments on three real-world traffic speed datasets and three real-world traffic flow datasets, respectively. The results show that LOCALEGN consistently outperforms other state-of-the-art baseline models for the few-shot traffic prediction. It is also demonstrated that the learned knowledge from LOCALEGN can be transferred across cities.

Source codes of LOCALEGN are publicly available at <https://github.com/MingxiLii/LocaleGN>. The remainder of this paper is organized as follows. Section II reviews the related studies on traffic prediction, few-shot learning, and graph neural networks. Section III formulates the task of few-shot traffic prediction and presents details of LOCALEGN. In Sections IV, numerical experiments are conducted to demonstrate the advantages of LOCALEGN. Lastly, conclusions and future research are summarized in Section V.

II. RELATED WORK

In this section, we first summarize the existing traffic prediction models, then applications of few-shot learning in transportation are discussed. Lastly, we review the emergence of GN and justify the choice of GN for few-shot traffic prediction.

1) *Traffic Prediction Models*: Traffic data as a spatio-temporal information on road networks (graphs) is a typical non-Euclidean data. There are two types of models to deal with

graph data: spatial graph-based models and spectral graph-based models [6]. In smart mobility applications, GCN is a widely used spectral graph-based model to learn the complex structure of spatio-temporal data, and the representative models include T-GCN [26], ST-GCN [27], TGC-LSTM [28], and ASTGCN [29]. The convolutional operation bases on the whole graph with its Laplacian matrix or other variants, such as dynamic Laplacian matrix [30]. However, the spectral graph-based models do not have parameter-sharing characteristics, thus these models are tied to specific graph topologies. For example, T-GCN and ST-GCN are inflexible and impose restrictions on transfer learning tasks across different graphs [31].

For spatial graph-based models, local aggregators are explored in order to deal with the direct convolution operation with the different number of neighbors [6]. In DCRNN [24], the bidirectional random walk is introduced to model the spatial correlation of traffic flow on graphs. In WAVENET, adaptive dependency matrix is adopted through the node embedding process, and the 1D convolution component is used to make the relation between entities trainable [25]. Moreover, attention-based spatial methods are developed to operate attention mechanism on graphs. In GATCN, the graph attention network is applied to extract the spatial features of the road network [32]. We note that existing spatial graph-based models have flexible graph representations but require large historical data to achieve a competitive accuracy. For example, in DCRNN, the pair-wise spatial correlation makes graph structures trainable, but its complex encoder and decoder structures also make the training data-intensive.

Methods mentioned above in the spectral and spatial domain mainly focus on modeling the spatial dependency of the traffic data. In addition to capturing spatial patterns, many other models are combined to learn temporal patterns. For example, Recurrent Neural Network (RNN) is adopted in time series prediction tasks [33, 34]. Both LSTM and GRU are two typical RNN models [35], and attention mechanism can also be used for inferring temporal dependencies (e.g., AST-GAT [36], attention with LSTM [37], and APTN [38]).

2) *Few-shot Learning in Transportation*: Few-shot learning has been developed to transfer the knowledge learned in the source domain (e.g., dataset, road, city) to the target domain [39, 40, 41]. Thus, it is a promising methodology to deal with the data inefficiency issue in the field of transportation. The existing few-shot learning models can be categorized into two types: one is the gradient-based models [42] and the other is the metric-based models [43]. These methodologies work well in the case of the independent and identically distributed data. However, few-shot learning in graphs is more challenging as the nodes and edges on the graph are connected and correlated with each other. Transportation data is a typical type of graph-based data. In recent years, studies explore the few-shot learning with transportation applications such as vehicle detection [44] and traffic sign recognition [45]. In traffic prediction tasks, region-based transfer learning across cities is applied by matching similar sub-regions among different cities [46]. Overall, explorations of few-shot learning for traffic prediction are still lacking.

3) *Graph Networks*: Spectral GCN models and spatial GNN models can be adopted for traffic prediction tasks [7]. The inflexibility of the former one makes it unfeasible to construct few-shot or transfer prediction models. Therefore, it is worthwhile to look into spatial-based GNN models. There are many popular spatial-based GNN models such as diffusion graph convolution (DGC) [47], MPNN [23], GRAPHsAGE [48], and graph attention networks (GAT) [49]. Traffic speed or flow prediction models base on DGC, MPNN, GRAPHsAGE and GAT for short-term prediction are developed with sufficient traffic data. However, these models may fail in the cases of few data samples. In view of this, we note that Graph Network (GN) with relational inductive biases could address the issue of data intensity. In [20], the relational inductive bias is widely discussed when utilizing deep learning models to deal with structured data. In recent years, GN has been used to simulate physical systems [50, 51], predict the structure in glassy systems [52], and simulate the molecular dynamic systems [53]. All these studies demonstrate the great potential of GN in modeling the localized relationship that is viewed as the relational inductive biases. Referring to spatio-temporal networks, GN is utilized to predict the climate data and the encoder-GN-decoder structure is developed to strengthen the representation ability in uncovering the complex and diverse connectivity of spatio-temporal networks [21]. Overall, it is worth exploring to extend GN to traffic prediction as the road network is also viewed as a typical spatio-temporal network.

III. MODEL

In this section, we formulate the few-shot traffic prediction task. The overall framework of LOCALEGN is presented and each component is introduced in detail. Lastly, the computational steps in LOCALEGN are summarized.

A. Few-shot Traffic Prediction

Traffic prediction task can be formulated as a regression problem. Various traffic data, such as traffic speed and flow, are graph-based, which can be modeled on a spatio-temporal graph. Different types of data might associate with nodes or edges. For example, the point detector data is associated with nodes, while the travel time data is associated with edges. We define the graph associated with the traffic data as a directed graph $\mathcal{G} = (\mathcal{V}, \mathcal{E})$, where each node is represented by i , and the set of node indices $\mathcal{V} = \{1, 2, \dots, i, \dots, N_v\}$. N_v is the number of traffic sensors. Similarly, the set of edges is defined as $\mathcal{E} = \{1, 2, \dots, k, \dots, N_e\}$, where N_e represents the number of edges. The connectivity among nodes and edges represents the relational inductive biases on the graph.

In this paper, we formulate the traffic prediction on time-dependent (dynamic) graphs. Suppose the set of time intervals during the study period is denoted as T , for each time interval τ , we define the time-dependent data on graph \mathcal{G} as $\mathbf{G}^\tau = (\mathbf{V}^\tau, \mathbf{E}^\tau)$, where $\mathbf{V}^\tau \in \mathbb{R}^{N_v \times T}$ and $\mathbf{E}^\tau \in \mathbb{R}^{N_e \times T}$. To be precise, $\mathbf{V}^\tau = [\mathbf{v}_1^\tau; \dots; \mathbf{v}_i^\tau; \dots; \mathbf{v}_{N_v}^\tau]$, and $\mathbf{v}_i^\tau = [v_i^{\tau-M}, \dots, v_i^\tau]^T \in \mathbb{R}^{1 \times M}$, where \mathbf{v}_i^τ represents the traffic data for node i at time τ . M is the look-back window. The edge-based data $\mathbf{E}^\tau = [\mathbf{e}_1^\tau; \dots; \mathbf{e}_k^\tau; \dots; \mathbf{e}_{N_e}^\tau]$,

and $\mathbf{e}_k^\tau = [e_k^{\tau-M}, \dots, e_k^\tau]^T$, where e_k^τ represents the traffic data on edge k at time τ . We note the time-dependent data in \mathbf{G}^τ can not only include conventional traffic data, but also other graph-based datasets such as weather, road properties, and so on. In this paper, without loss of generality, we suppose the nodes carry the point detector data, while the edges include the road properties (e.g., length, width, category).

Based on the above notations, existing traffic prediction models can be viewed as a function Φ , and $\Phi(\mathbf{G}^\tau) = \mathbf{V}^{\tau+1}$. Φ can be viewed as a dynamical system that evolves the graph-based traffic data from time τ to $\tau + 1$. For each τ , suppose \mathbf{G}^τ follows a certain distribution \mathcal{D} , then we have $\mathbf{G}^\tau \sim \mathcal{D}$. Given a sufficient large T , it is expected that we can use the deep learning model to approximate Φ such that the prediction error $\|\hat{\Phi}(\mathbf{G}^\tau) - \mathbf{V}^{\tau+1}\|$ is minimized, where $\hat{\Phi}$ represents the deep learning-based approximator.

In the few-shot traffic prediction task, the set of archived time interval T is relatively small, say $|T| = 10$, and then training $\hat{\Phi}$ can easily overfit, making the existing traffic prediction models not suitable for the few-shot tasks. To address this issue, we propose to develop a function $\Psi(\mathbf{v}_i^\tau, \mathcal{L}^\tau(i)) = v_i^{\tau+1}, \forall i$, where $\mathcal{L}^\tau(i)$ represents the locale of node i at time τ . For example, $\mathcal{L}(i)^\tau$ can represent all the \mathbf{e}_k and \mathbf{v}_i that are within the K -hop neighborhoods of node i . To obtain an approximator of Ψ , we notice that the available number of training data becomes $|T|N_v$. If the deep learning-based approximator $\hat{\Psi}$ could learn the *locally spatial* and temporal pattern for each node with $|T|N_v$ number of samples, then the few-shot traffic prediction task can be solved. In the following sections, we present and validate LOCALEGN as a suitable selection for $\hat{\Psi}$.

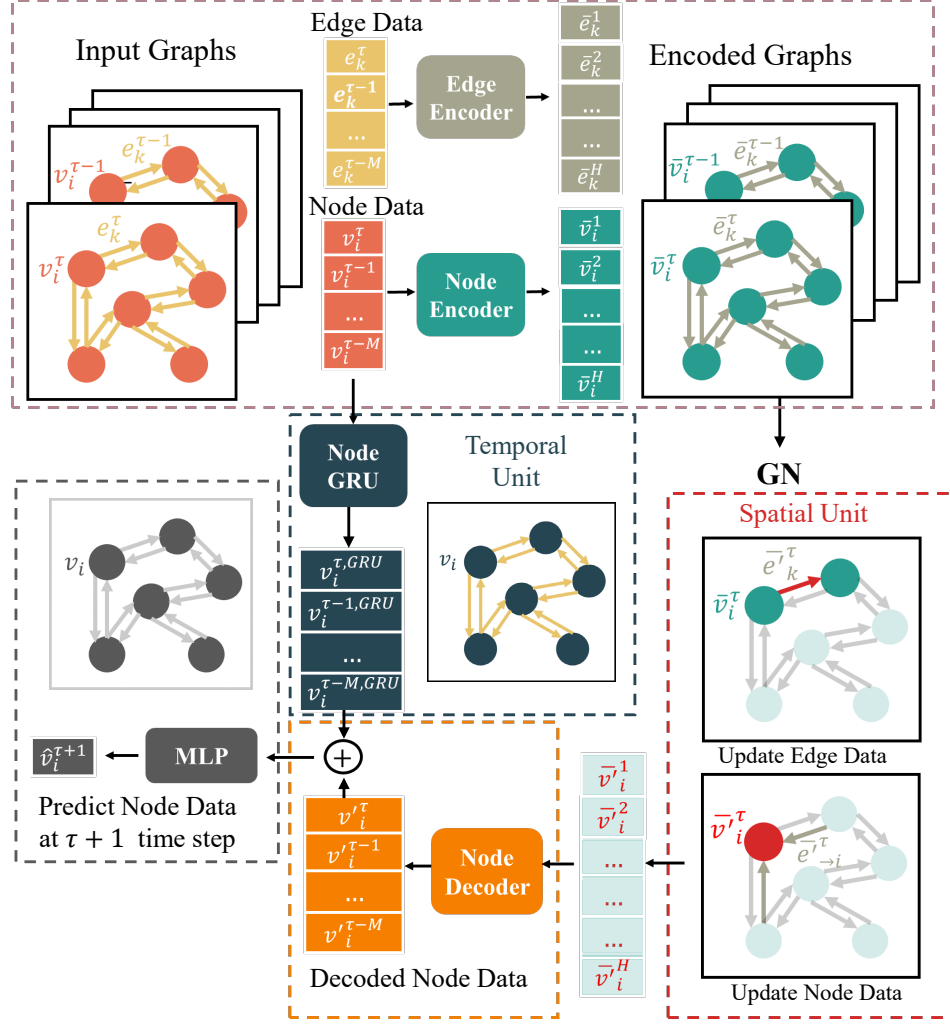
B. LOCALEGN

In this section, we introduce LOCALEGN in detail. Firstly, an overview of LOCALEGN is shown in Figure 4.

LOCALEGN mainly consists of four major components: node Gate Recurrent Unit (NODEGRU), node and edge encoders, graph network (GN) and nodes decoder. At each time τ , the input of LOCALEGN is \mathbf{G}^τ , and the node data \mathbf{V}^τ is feed into the NODEGRU for learning the temporal patterns of each node. Simultaneously, both edge data \mathbf{E}^τ and node data \mathbf{V}^τ are embedded by the edge encoder and node encoder, respectively. The GN is used to model the *locally spatial* patterns on both nodes and edges, and the edge information is aggregated to nodes. Then, the aggregated node information is further decoded by the node decoder. Lastly, the temporal patterns by NODEGRU is concatenated with the *locally spatial* patterns by GN, and a dense layer is used to generate the final prediction for $\mathbf{v}_i^{\tau+1}, \forall i$.

1) NODEGRU: The NODEGRU focuses on capturing the temporal correlation on \mathbf{v}_i for each node separately, as presented in Equation 1. The temporal pattern of \mathbf{v}_i is embedded in the GRU, which will be used for the inference of time $\tau + 1$ in the following steps. We note that the GRU is applied for each node separately, which makes the trainable parameters dependent on the network size.

$$\mathbf{v}_i^{\tau, \text{GRU}} = \text{GRU}(\mathbf{v}_i^\tau), \forall i, \tau \quad (1)$$

Fig. 4: An overview of LOCALEGN (H represents the size of hidden layers).

2) *Node and Edge Encoder*: To encode the node and edge data in \mathbf{G}^τ , we employ two multilayer perceptron MLP^E and MLP^V for edge and node respectively, as shown in Equation 2.

$$\begin{aligned} \bar{\mathbf{e}}_k^\tau &= \text{MLP}^E(\mathbf{e}_k^\tau), \forall k, \tau \\ \bar{\mathbf{v}}_i^\tau &= \text{MLP}^V(\mathbf{v}_i^\tau), \forall i, \tau \end{aligned} \quad (2)$$

The encoded node and edge data can form the encoded graph $\bar{\mathbf{G}}^\tau = (\bar{\mathbf{V}}^\tau, \bar{\mathbf{E}}^\tau)$. In general, the two encoders can better learn the latent representations of these node and edge data, and the learned representations will be used to further mine the spatial and temporal relationship by GN.

3) *Graph Network*: The graph network (GN) is the essential component in LOCALEGN. In general, GN models the evolution of dynamic graphs using the updating and aggregating operations on nodes and edges. In particular, we aim to use GN to evolve $\bar{\mathbf{G}}^\tau$ to $\bar{\mathbf{G}}^{\tau+1}$.

In GN, two updating functions ϕ^V, ϕ^E are employed to update the per-node data and per-edge data respectively, and one aggregating function $\rho^{E \rightarrow V}$ is used to aggregate the per-edge data for each node. To provide more details, GN models the spatio-temporal propagation of the dynamic graph $\bar{\mathbf{G}}^\tau$ based on the following three steps:

i In the first step, the edge updating function ϕ^E is applied to every single edge in the graph to calculate the per-edge updates. For each edge k , we combine the updated edge data $\bar{\mathbf{e}}_k^\tau$ and the node data for both the tail node $\text{tail}(k)$ and head node $\text{head}(k)$ of k , and then the combined data is feed into ϕ^E , as shown in the following equation:

$$\bar{\mathbf{e}}_k^\tau = \phi^E(\bar{\mathbf{e}}_k^\tau, \bar{\mathbf{v}}_{\text{tail}(k)}^\tau, \bar{\mathbf{v}}_{\text{head}(k)}^\tau), \forall k, \tau, \quad (3)$$

where ϕ^E is modeled through an MLP (MLP^{ϕ^E}).

ii In step two, the aggregating function $\rho^{E \rightarrow V}$ is applied to all the edges that point to node i . Mathematically, we denote $\bar{\mathbf{E}}_{\rightarrow i}^\tau = \{\bar{\mathbf{e}}_k^\tau | \text{tail}(k) = i, \forall k\}$ as the set of the updated edge data pointing to i at time τ . The function $\rho^{E \rightarrow V}$ aggregates the information in $\bar{\mathbf{E}}_{\rightarrow i}^\tau$ and outputs a representation of all the edges pointing to node i , as shown in Equation 4. We note that the aggregating function should work on different size of $\bar{\mathbf{E}}_{\rightarrow i}^\tau$, and hence the element-wise mean function is chosen as $\rho^{E \rightarrow V}$.

$$\bar{\mathbf{e}}_{\rightarrow i}^\tau = \rho^{E \rightarrow V}(\bar{\mathbf{E}}_{\rightarrow i}^\tau), \forall i, \tau \quad (4)$$

iii In step three, the node updating function ϕ^V is applied to every single node in the graph. For node i , the function ϕ^V

takes the current node data $\bar{\mathbf{v}}_i^\tau$ and the representation of the edge data pointing to node i computed in the previous step as input, and the output is the updated node data \mathbf{v}'_i^τ , as represented in the following equation:

$$\mathbf{v}'_i^\tau = \phi^V(\bar{\mathbf{e}}_{\rightarrow i}^\tau, \bar{\mathbf{v}}_i^\tau), \forall i, \tau, \quad (5)$$

where ϕ^V is modeled as a different MLP (MLP^{ϕ^V}).

Overall, the GN model decomposes the complex topological graph structure into updating and aggregating operations on each single node and edge, and the localized relationship on the graph can be modeled accordingly. Indeed, the updating and aggregating operations in GN mimic the localized traffic exchanges shown in Figure 3, and hence it is powerful in uncovering the *locally spatial* patterns of traffic data. Additionally, GN is applied to each node and edge separately, so it is independent of network size, which is another attractive feature of GN.

4) *Node Decoder*: The updated node $\bar{\mathbf{v}}_i^\tau$ from the GN model is further decoded by the node decoder. Similar to the node encoder, the node decoder is modeled through an MLP, as shown in Equation 6.

$$\mathbf{v}'_i^\tau = \text{MLP}^{V'}(\bar{\mathbf{v}}_i^\tau), \forall i, \tau \quad (6)$$

where \mathbf{v}'_i^τ represents the decoded data for node i at time τ .

5) *Output Layer*: In the output layer, we combine the *locally spatial* and temporal information obtained from the NODEGRU and node decoder, respectively. Mathematically, we concatenate $\mathbf{v}_i^{\tau, \text{GRU}}$ and \mathbf{v}'_i^τ , the resulting vector is feed into an MLP for predicting the traffic states at time $\tau + 1$, as shown in Equation 7.

$$\hat{v}_i^{\tau+1} = \text{MLP}^{\text{Output}}(\mathbf{v}'_i^\tau \oplus \mathbf{v}_i^{\tau, \text{GRU}}), \forall i, \tau \quad (7)$$

where \oplus is the vector concatenation operator, $\hat{v}_i^{\tau+1}$ is the prediction for $v_i^{\tau+1}$, and $\text{MLP}^{\text{Output}}$ represents another MLP. To summarize, all the computational steps in the LOCALEGN are presented in Algorithm 1.

Finally, the difference between the prediction $\hat{v}_i^{\tau+1}$ and the actual data $v_i^{\tau+1}$ is measured by the ℓ_2 norm represented by $\sum_i (v_i^{\tau+1} - \hat{v}_i^{\tau+1})^2$. The error is back-propagated to update all the parameters in LOCALEGN.

C. Transferability of LOCALEGN

In this section, we discuss how LOCALEGN is different from the existing traffic prediction models in terms of transferability. The most important feature of LOCALEGN is that both GN and NODEGRU modules make use of the parameter sharing characteristic so that the knowledge learned for traffic prediction can be transferred among nodes. Though most of the existing GNNS can be cast into the message passing neural networks and hence the parameters can be shared [23], existing traffic prediction models avoid using the parameter sharing characteristic because it could impede the prediction performance.

In this study, we particularly consider the edge data \mathbf{e}_i^τ , which represents road properties (e.g., road length, width, and

Algorithm 1 Computational steps in LOCALEGN.

Require: graph structure $\mathcal{G} = (\mathcal{V}, \mathcal{E})$, node data $\mathbf{V}^\tau = [\mathbf{v}_1^\tau; \dots; \mathbf{v}_i^\tau; \dots; \mathbf{v}_{N_v}^\tau]$ and edge data $\mathbf{E}^\tau = [\mathbf{e}_1^\tau; \dots; \mathbf{e}_k^\tau; \dots; \mathbf{e}_{N_e}^\tau]$.

Ensure: GRU in Equation 1, MLP^E and MLP^V in Equation 2, MLP^{ϕ^E} and MLP^{ϕ^V} in GN, $\text{MLP}^{V'}$ in Equation 6, and $\text{MLP}^{\text{Output}}$ in Equation 7 are properly initialized and trained.

for $i \in \{1, \dots, N^v\}$ **do**

- Compute $\mathbf{v}_i^{\tau, \text{GRU}}$ based on Equation 1.
- Compute $\bar{\mathbf{v}}_i^\tau$ based on Equation 2.

end for

for $k \in \{1, \dots, N^e\}$ **do**

- Compute $\bar{\mathbf{e}}_k^\tau$ based on Equation 2.
- Update the edge data using the edge updating function based on Equation 3.

end for

for $i \in \{1, \dots, N^v\}$ **do**

- Form the set of the updated edges pointing to node i as $\bar{\mathbf{E}}_{\rightarrow i}^\tau$.
- Compute $\bar{\mathbf{e}}_{\rightarrow i}^\tau$ based on Equation 4 and $\bar{\mathbf{E}}_{\rightarrow i}^\tau$.
- Compute $\mathbf{v}_i^{\tau, \text{GRU}}$ based on Equation 5.
- Decode the updated node data based on Equation 6.
- Concatenate $\mathbf{v}_i^{\tau, \text{GRU}}$ and $\mathbf{v}_i^{\tau, \text{GRU}}$.
- Predict $\hat{v}_i^{\tau+1}$ based on Equation 7.

end for

return $\hat{v}_i^{\tau+1}, \forall i \in \{1, \dots, N^v\}$

types), location information (e.g., weather, socio-demographic factors), and so on. For node i , we define the locale of node i at time τ to be $\mathcal{L}^\tau(i) = \{\mathbf{v}_i^\tau, \bar{\mathbf{E}}_{\rightarrow i}^\tau\}$, and hence the information contained in the locale can be used to conduct traffic prediction independently. The learning of traffic states becomes inductive, *i.e.*, LOCALEGN universally learns the traffic states conditional on the locale, instead of learning the traffic states for each node separately. Later in the experimental experiments, we demonstrate that with the consideration of edge data, the node embedding can be learned through a universal encoder, *i.e.*, the GN module, and the traffic prediction can be conducted per node. Additionally, the information contained in the locale is permutation-invariant, hence LOCALEGN is suitable for different network topologies for traffic prediction.

D. Determining the number of GN layers

One can see that the GN (spatial unit) in LOCALEGN depicts the traffic states on each node, and the K layers of GN can be stacked to model the localized traffic exchanges for the K -hop neighbors. In this section, we discuss how to determine K with theoretical analysis.

In general, traffic states are formed through the traffic flow forward propagation and congestion spillover. To predict traffic states on node i for the next h minutes, we should ensure that the traffic exchanges in the next h minutes are within the K -hop neighbors, so that GN has the capability to capture the changes in traffic states. Without loss of generality, we assume that around node i , the free flow speed is v and the shockwave speed is w , respectively. We define $d_i(j), \forall j \in \mathcal{V}$,

which represents the distance from node i to node j , and K can be determined using Equation 8.

$$\begin{aligned} K &= \max \cup_{i \in \mathcal{V}} [\mathcal{I}_i^{\text{forward}} \cup \mathcal{I}_i^{\text{backward}}] \\ \mathcal{I}_i^{\text{forward}} &= \{ \text{hop}_i(j) | d_i(j) \leq hv, \forall j \in \mathcal{V} \} \\ \mathcal{I}_i^{\text{backward}} &= \{ \text{hop}_j(i) | d_j(i) \leq hw, \forall j \in \mathcal{V} \} \end{aligned} \quad (8)$$

where $\text{hop}_i(j)$ counts the number of edges in the shortest path from i to j . $\mathcal{I}_i^{\text{forward}}$ and $\mathcal{I}_i^{\text{backward}}$ denote the sets of edge numbers to which the forward traffic flow and congestion spillover could reach from node i , respectively. Using Figure 5 as an example, the impact of a source node can spread to its directly connected neighbors in 5 minutes. It will take longer time to spread the impact further and hence it suffices to consider a small number of K based on Equation 8.

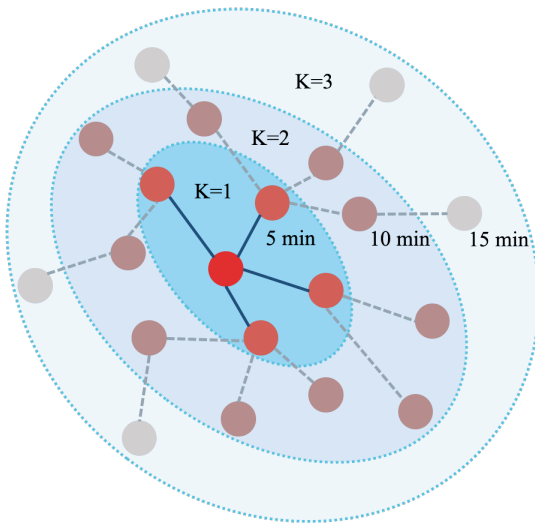


Fig. 5: Determining the number of GN layers.

IV. NUMERICAL EXPERIMENTS

In this section, the proposed model is examined in real-world flow and speed datasets to test the short-term prediction performance.

A. Datasets

We evaluate LOCALEGN and other baseline models on three traffic speed and three traffic flow datasets, respectively. The detailed dataset information is listed as follows:

1) *Traffic Speed Data*: Three speed datasets are used and the time interval is every five minutes:

- LA: The LA dataset is collected from 207 loop detectors in Los Angeles, and the data ranges from March 1st to March 7th, 2012.
- SacS: also known as PEMSD7, which contains speed data from 228 detectors in the Sacramento area. The data ranges from May to June, 2012.
- ST: ST contains speed data from 170 sensors in the Seattle Area. The data ranges from Jan 1st to Feb 1st, 2015.

2) *Traffic Flow Data*: Three traffic flow datasets in [54] are utilized and the time interval is every five minutes:

- SF: also known as PEMS04, which includes 307 sensors in the San Francisco Bay area, and the data ranges from September 1st to November 7th, 2018.
- SacF: also known as PEMS07, which contains traffic flow data from 883 detectors in the Sacramento area. The data ranges from January 1st to August 7th, 2018.
- SanB: also known as PEMS08, which contains traffic flow data from 170 sensors in the San Bernardino area, and the data ranges from July 1st to August 7th, 2016.

B. Baseline models

The following baseline models will be compared with LOCALEGN. Particularly, NODEGRU and GN are presented for ablation study.

- GCN: Graph Convolutional Network for graph-based data prediction [55].
- LSTM: Long Short-Term Memory network for time series prediction [56].
- T-GCN: Temporal Graph Convolutional Network [57]. Spatial dependency is captured by the GCN module and temporal correlation is abstracted by GRU.
- ST-GCN: Spatial-Temporal Graph Convolutional Network [27]. ChebNet and 2D convolutional network are utilized to capture the spatial and temporal correlation, respectively.
- DCRNN: Diffusion Convolutional Recurrent Neural Network [24].
- WAVENET: Graph WaveNet for Deep Spatial-Temporal Graph Modeling [25].
- NODEGRU: Gated Recurrent Unit [58] for every single node's data in graph. This model can be viewed as LOCALEGN with only GRU component.
- GN: Graph network model with relational inductive bias [24]. This model can be viewed as LOCALEGN without the NODEGRU module.

C. Experimental Settings

All experiments are conducted on a desktop with Intel Core i9-10900K CPU @3.7GHz × 10, 2666MHz × 2 × 16GB RAM, GeForce RTX 2080 Ti × 2, 500GB SSD. We divide all speed and flow datasets of seven days with ratio of 6 : 1 : 1 into training set, validation set and testing set. Since the most commonly used historical data ranges from 7 days to 30 days, we choose 7 days' data as the minimum sufficient data for training of the most majority of existing prediction model. To simulate the situation of limited training samples, we randomly select 20% of the training set for training. When constructing \mathbf{G}^T , we set the edge data to be the normalized distance of the edges between two nodes, and the node data are the traffic speed or traffic flow from different datasets. We use one hour historical data to predict the next five minutes' data, meaning $M = 12$. Hyper-parameters in LOCALEGN are determined by the validation set, and the finalized model specifications are presented in Appendix A.

D. Evaluation Metrics

Three different metrics are chosen to evaluate the prediction performance of LOCALEGN and other baseline models by comparing $\hat{v}_i^{\tau+1}$ with the ground truth $v_i^{\tau+1}$.

- Root Mean Squared Error (RMSE):

$$\text{RMSE} = \sqrt{\frac{1}{N^v} \sum_{i=1}^{N^v} (\hat{v}_i^{\tau+1} - v_i^{\tau+1})^2}$$
- Mean Absolute Error (MAE):

$$\text{MAE} = \frac{1}{N^v} \sum_{i=1}^{N^v} |\hat{v}_i^{\tau+1} - v_i^{\tau+1}|$$
- Mean Absolute Percentage Error (MAPE):

$$\text{MAPE} = \frac{100\%}{N^v} \sum_{i=1}^{N^v} \left| \frac{\hat{v}_i^{\tau+1} - v_i^{\tau+1}}{v_i^{\tau+1}} \right|$$

E. Experimental Results

Table I and Table II present the prediction accuracy of different models with few training samples on three speed and flow datasets, respectively. One can see the proposed LOCALEGN model consistently outperforms other baseline models on six datasets. LSTM utilizes temporal correlations, and GCN models the spatial dependencies; both models cannot fully take the spatio-temporal dependencies into consideration at the same time. With few training samples, the performance of the state-of-the-art models like T-GCN and ST-GCN degrades, while LOCALEGN achieves higher prediction accuracy. Among parameters-sharing models, LOCALEGN also outperforms DCRNN and WAVENET. It is probably due to the complicated encoder and decoder structure of DCRNN and the specified node embedding of WAVENET. The complicated structures make them overfit the limited available data. However, with parameters-sharing characteristic, LOCALEGN is a light-weighted model with the well-designed structure that perfectly meets the requirements of short-term traffic prediction with few samples.

We note for the flow datasets, the standard deviation is high for the baseline models, which suggests that these model may overfit with few training samples. Besides, there is a large gap between the prediction accuracy of NODEGRU and LSTM, although GRU and LSTM are similar RNN modules. It is because the complicated model is inclined to overfit on small datasets. GRU is less complicated than LSTM and LSTM is applied for all nodes' data while NODEGRU is for single node separately, which means LSTM have more trainable parameters and more complicated.

1) *Ablation Study*: The ablation study has been included in Table I and Table II by comparing with NODEGRU and GN, as both models are the essential components of LOCALEGN. In speed datasets, we observe that LOCALEGN is consistently better than the other two models. In flow datasets, NODEGRU and GN occasionally outperform LOCALEGN, which suggests that either the GRU component or GN component might dominate for a specific dataset. Overall, LOCALEGN achieves satisfactory performance for all datasets under different metrics.

2) *Justifying the use of each module*: We further conduct more experiments to justify the use of NODEGRU and GN. To this end, we try to replace each module with other modules with similar functionality. For example, NODEGRU can be replaced with a residual connection [59], and GN can be

replaced with a self-attention module [60]. We find that both NODEGRU and GN outperform their counterparts, which justifies the use of both modules. Details are presented in Appendix B.

F. Number of Model Parameters

According to the few-shot experiments results, although inferior to LOCALEGN, ST-GCN achieves better prediction accuracy than other baseline models. We compare the number of trainable parameters of LOCALEGN and ST-GCN in Table III. For any network of arbitrary size, the number of trainable parameters in LOCALEGN remains the same. However, for ST-GCN, the number of its parameters is positively correlated with the network size. For example, the flow dataset SacF has a large node number of 883, and the number of trainable parameters in ST-GCN is ten times larger than that of LOCALEGN. However, the prediction performance of LOCALEGN is even better than that of ST-GCN. It further proves that the short-term traffic prediction relies on localized information, and this can be efficiently learned from few samples with graph relational inductive biases.

In traditional graph model for spatio-temporal data prediction, the parameters sets are different for different nodes and it causes the difficulty for the training process of large graphs. However, LOCALEGN makes it feasible to learn across nodes. It can be seen as the transfer learning model among different nodes on a network. One node and its neighborhoods can be interpreted as a sub-graph, and LOCALEGN is able to extract useful information from the sub-graphs. This suggests the reason why LOCALEGN requires fewer samples for training.

G. Sensitivity Analysis

Apart from evaluation in few training samples (20% of the training data), we also compare the prediction performance of LOCALEGN and other baseline models with different percentages of training data (from 20% to 100%), the results are presented in Figure 6. The prediction performance remains stable for LOCALEGN when the training ratio decreases from 100% to 20%, while the prediction performance of ST-GCN gradually degrades when reducing the number of training samples.

Overall, LOCALEGN outperforms T-GCN and ST-GCN with all percentages of training data and the advantage is notably large when the ratio is 20% or 40%. In other words, T-GCN and ST-GCN overfit and become unstable when the training set is small. In contrast, LOCALEGN has better learning ability in capturing the localized spatial and temporal correlations than T-GCN and ST-GCN. The results further demonstrate that LOCALEGN is a powerful and efficient model for the task of the few-shot traffic prediction.

H. Cross-city Transfer Analysis

In this section, we consider a more challenging situation, in which traffic sensors are just installed or the traffic prediction service is just deployed in a city. In this case, we would like to use the knowledge learned from some city and directly apply

TABLE I: Performance of LOCALEGN and other baseline models on traffic speed datasets (average \pm standard deviation across 5 experimental repeats; unit for RMSE and MAE: miles/hour).

Model	LA			SacS			ST		
	RMSE	MAPE (%)	MAE	RMSE	MAPE (%)	MAE	RMSE	MAPE (%)	MAE
GCN	11.99 \pm 1.02	28.77 \pm 3.44	8.55 \pm 0.65	11.68 \pm 0.05	24.0 3 \pm 0.17	7.96 \pm 0.15	9.54 \pm 0.10	19.93 \pm 0.21	6.99 \pm 0.12
LSTM	12.78 \pm 0.04	29.88 \pm 0.40	9.34 \pm 0.08	11.89 \pm 0.19	23.12 \pm 0.65	8.28 \pm 0.08	9.94 \pm 0.06	20.44 \pm 0.16	6.70 \pm 0.13
T-GCN	5.93 \pm 0.72	10.44 \pm 1.80	4.02 \pm 0.51	4.05 \pm 0.91	5.42 \pm 1.32	2.25 \pm 0.49	5.09 \pm 0.49	8.10 \pm 0.86	3.40 \pm 0.27
ST-GCN	5.47 \pm 0.25	10.39 \pm 1.01	3.46 \pm 0.18	5.50 \pm 0.50	9.54 \pm 1.14	3.09 \pm 0.27	4.38 \pm 0.05	6.75 \pm 0.10	2.86 \pm 0.03
DCRNN	5.97 \pm 0.39	11.11 \pm 0.93	4.45 \pm 0.39	8.42 \pm 0.69	15.38 \pm 1.50	5.53 \pm 0.69	5.49 \pm 0.87	9.24 \pm 1.97	3.92 \pm 0.87
WAVENET	10.11 \pm 0.54	24.09 \pm 1.32	6.72 \pm 0.30	9.30 \pm 1.00	19.06 \pm 2.09	6.16 \pm 0.58	7.83 \pm 0.78	15.83 \pm 1.70	5.15 \pm 0.48
GN	4.44 \pm 0.10	7.15 \pm 0.28	2.86 \pm 0.19	2.84 \pm 0.12	4.10 \pm 0.13	1.81 \pm 0.08	4.15 \pm 0.03	6.14 \pm 0.03	2.77 \pm 0.02
NODEGRU	4.72 \pm 0.10	7.82 \pm 0.36	2.92 \pm 0.14	3.48 \pm 0.17	4.87 \pm 0.39	2.16 \pm 0.18	4.29 \pm 0.05	6.59 \pm 0.22	2.81 \pm 0.05
LOCALEGN	4.24 \pm 0.05	6.88 \pm 0.22	2.70 \pm 0.05	2.56 \pm 0.08	3.72 \pm 0.29	1.65 \pm 0.11	4.00 \pm 0.02	5.96 \pm 0.12	2.65 \pm 0.01

TABLE II: Performance of LOCALEGN and other baseline models on traffic flow datasets (average \pm standard deviation across 5 experimental repeats; unit for RMSE and MAE: vehicles/hour).

Model	SF			SacF			SanB		
	RMSE	MAPE (%)	MAE	RMSE	MAPE (%)	MAE	RMSE	MAPE (%)	MAE
GCN	74.48 \pm 57.97	90.05 \pm 912.20	93.04 \pm 57.97	105.74 \pm 54.29	519.16 \pm 143.94	130.18 \pm 143.94	70.82 \pm 72.28	153.15 \pm 31.56	89.32 \pm 31.56
LSTM	63.19 \pm 1.21	924.73 \pm 45.93	44.79 \pm 1.01	92.73 \pm 0.95	414.45 \pm 14.19	65.87 \pm 1.27	576.38 \pm 0.55	103.77 \pm 1.49	57.66 \pm 0.60
T-GCN	29.58 \pm 3.04	210.71 \pm 64.90	19.74 \pm 2.65	34.86 \pm 2.63	49.41 \pm 15.23	22.51 \pm 2.31	31.68 \pm 3.34	50.19 \pm 2.66	21.67 \pm 2.69
ST-GCN	34.10 \pm 1.23	219.10 \pm 11.24	23.19 \pm 0.82	59.77 \pm 6.78	86.98 \pm 14.59	42.76 \pm 5.09	31.59 \pm 0.74	42.29 \pm 0.83	21.20 \pm 0.55
DCRNN	92.89 \pm 6.77	665.33 \pm 140.92	67.57 \pm 6.77	101.73 \pm 12.43	513.67 \pm 64.71	78.90 \pm 12.43	95.07 \pm 9.25	354.90 \pm 36.97	73.11 \pm 9.25
WAVENET	81.54 \pm 13.56	99.00 \pm 20.35	65.10 \pm 11.30	116.40 \pm 7.75	140.46 \pm 14.88	97.43 \pm 6.70	99.82 \pm 7.42	134.67 \pm 26.35	81.98 \pm 5.20
GN	25.61 \pm 0.41	30.96 \pm 2.77	17.84 \pm 0.41	30.52 \pm 0.42	14.65 \pm 2.49	19.77 \pm 0.57	28.52 \pm 1.65	16.54 \pm 0.94	19.85 \pm 1.54
NODEGRU	25.27 \pm 0.66	28.43 \pm 11.10	17.75 \pm 1.00	32.84 \pm 2.44	15.05 \pm 11.32	22.57 \pm 3.40	28.12 \pm 0.74	13.07 \pm 0.78	19.57 \pm 0.74
LOCALEGN	25.08 \pm 0.85	23.12 \pm 6.09	17.26 \pm 0.07	30.70 \pm 1.04	10.53 \pm 4.34	20.03 \pm 0.74	26.74 \pm 0.74	14.86 \pm 3.75	18.43 \pm 0.64

TABLE III: Comparison of the number of trainable parameters between ST-GCN and LOCALEGN (Unit: in thousand).

Model	Number of Trainable Parameters		
	LA	SacS	ST
ST-GCN	459	516	827
LOCALEGN	346	346	346
	SF	SacF	SanB
ST-GCN	768	4,493	371
LOCALEGN	346	346	346

it to a new city. To this end, we consider one city (target graph) that does not have historical traffic data, while some other cities (source graphs) have archived historical data. One can see this setting focuses on the transfer learning across cities. The well-performed LOCALEGN model is designed for extracting locally spatial and temporal traffic patterns, which is independent of graph structures and has the potential to be transferred to the target city. As the spectral graph-based GNN can be applied to graph structures, we compare LOCALEGN with DCRNN and WAVENET, the two state-of-the-art spectral graph-based models.

We compare the three models on speed and flow datasets respectively. Each model is pre-trained on a source graph with a random 20% of the training data and then directly tested on the target graph without further training. The prediction results on the target graph are presented in Table IV and Table V. One can see that LOCALEGN consistently outperforms DCRNN and WAVENET on different cities for both speed and flow datasets, and the prediction accuracy is very stable. The results show that LOCALEGN has great potential to transfer pre-trained models across cities even without fine-tuning the data of the target city because the universal traffic patterns and physical rules regardless of network structures can be learned

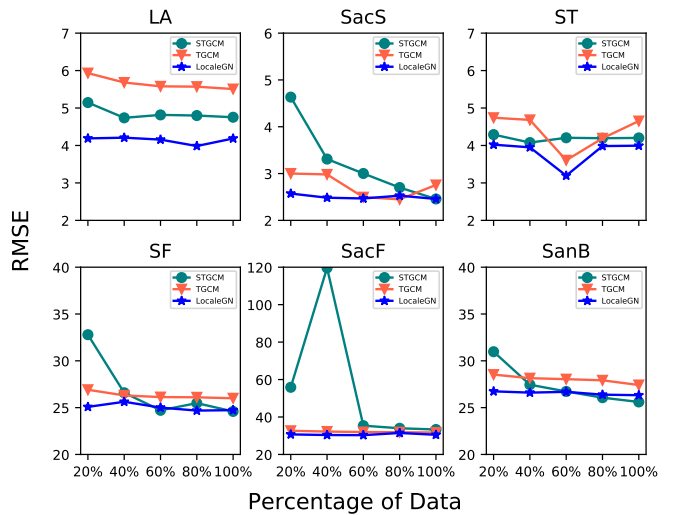


Fig. 6: Comparison of prediction performance among LOCALEGN, T-GCN and ST-GCN with the percentage of training set ranging from 20% to 100% (first row: speed data LA, ST, and SacS, unit: miles/hour; second row: flow data SF, SacF, and SanB, unit: vehicles/hour).

by LOCALEGN.

In Figure 7, we compare the prediction results of WAVENET and LOCALEGN from 8:00 AM to 20:00 PM for three traffic speed datasets and three traffic flow datasets, respectively. In general, LOCALEGN can make more accurate predictions than WAVENET in all datasets. It is notable that when the speed/flow surges or decreases sharply, the performance of WAVENET will decline significantly while the prediction of LOCALEGN remains stable. This demonstrates that although

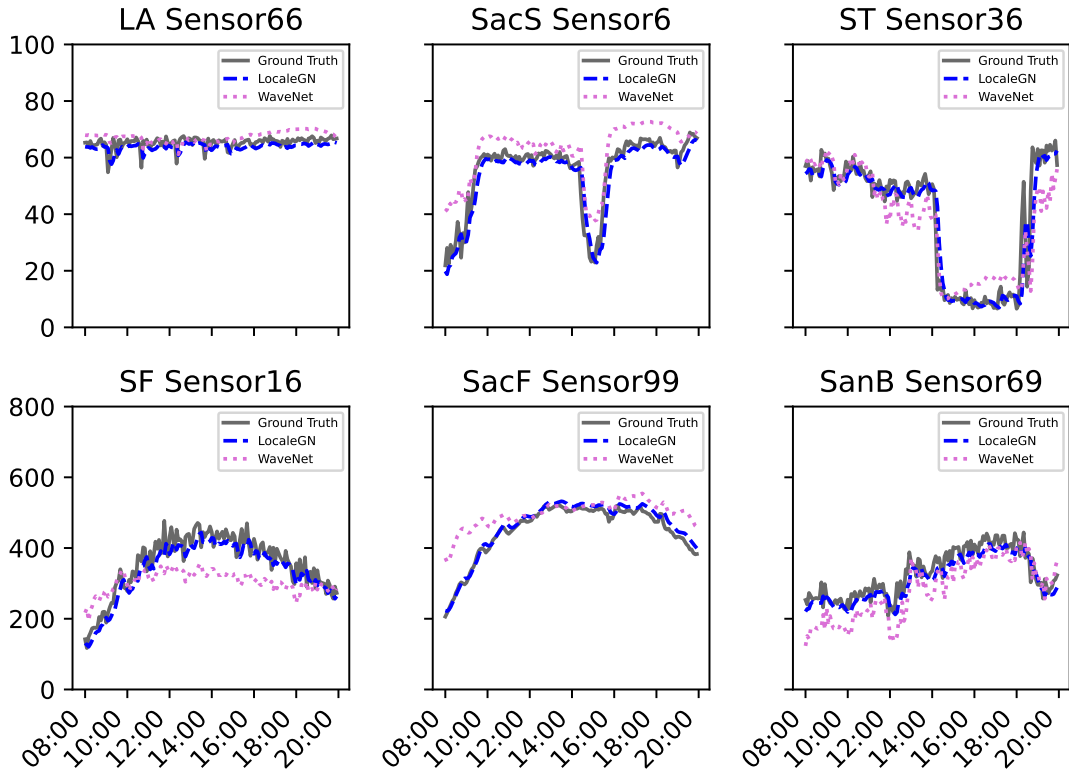


Fig. 7: Comparison of prediction performance with LOCALEGN and WAVENET for cross-city transfer analysis (first row: speed data LA, SacS, and ST, unit: miles/hour; second row: flow data SF, SacF, and SanB, unit: vehicles/hour).

WAVENET and DCRNN contain the parameters-sharing characteristics, they cannot learn the universal rule for short-term traffic prediction and their performance still depends on graph structures. Consequently, directly applying WAVENET and LOCALEGN to the target city will result in low prediction accuracy. In contrast, the performance of LOCALEGN remains satisfactory. The structure of LOCALEGN can serve as an essential building block for transferring prediction models between cities. Besides, the embedding and temporal components can be easily replaced with other state-of-the-art deep learning modules.

V. CONCLUSION

In this paper, we discuss and define the research question of few-shot traffic prediction on large-scale networks. A graph network-based model LOCALEGN is developed to learn the *locally spatial* and temporal patterns of traffic data, thus accurate short-term predictions can be generated. The parameter-sharing characteristics help LOCALEGN prevent overfitting with limited training data. Additionally, the learned knowledge in LOCALEGN can be transferred across cities. Extensive evaluations on six real-world traffic speed or flow datasets demonstrate that LOCALEGN outperforms other baseline models. LOCALEGN is also more light-weighted as it contains less trainable parameters, and this also suggests a shorter training time and lower data requirements. Ablation study and sensitivity analysis are conducted to show the compactness and robustness of LOCALEGN. The cross-city transfer analysis also

demonstrates its great potential in developing traffic prediction services without training in a new city. Overall, this paper sheds light on utilizing the transferability of LOCALEGN for traffic prediction and developing traffic prediction models for cities with few historically archived data.

As for the future research directions, firstly, it is necessary to interpret the knowledge learned by the LOCALEGN among different nodes, as this paper has demonstrated that the learned knowledge among nodes can contribute to the prediction accuracy. Secondly, because LOCALEGN can be applied to different cities, it is interesting to develop a unified and fair framework for training and testing the LOCALEGN on multiple cities without biases. Essentially, LOCALEGN has capacities in transferring knowledge not only among nodes in a single graph, but also across different graphs. Thirdly, LOCALEGN can be further extended to predict OD demand for public transit and ride-hailing services [61, 62]. Indeed, the enlightening idea of relational inductive bias and the simple structure of LOCALEGN can be applied to learn various spatio-temporal datasets, and the localized patterns can be extracted. These datasets include human mobility patterns, social media, epidemics, and climate-related data.

ACKNOWLEDGMENTS

The work described in this paper was supported by the National Natural Science Foundation of China (No. 52102385), a grant from the Research Grants Council of the Hong Kong Special Administrative Region, China (Project No.

TABLE IV: Transferring Performance of DCRNN, WAVENET and LOCALEGN on traffic speed datasets (average \pm standard deviation across 5 experimental repeats; unit for RMSE and MAE: miles/hour).

Source/Target	DCRNN			WAVENET			LOCALEGN		
	RMSE	MAPE (%)	MAE	RMSE	MAPE (%)	MAE	RMSE	MAPE (%)	MAE
LA/SacS	4.52 \pm 0.39	7.56 \pm 0.74	3.30 \pm 0.39	7.34 \pm 0.65	13.73 \pm 1.48	5.88 \pm 0.65	3.84 \pm 0.31	5.56 \pm 0.69	2.79 \pm 0.47
LA/ST	4.93 \pm 0.37	7.87 \pm 0.74	3.71 \pm 0.37	6.59 \pm 0.20	10.12 \pm 0.77	4.89 \pm 0.20	4.00 \pm 0.02	5.96 \pm 0.12	2.65 \pm 0.01
SacS/LA	9.90 \pm 1.20	19.93 \pm 2.46	6.57 \pm 1.20	7.15 \pm 0.32	13.20 \pm 1.51	5.06 \pm 0.32	5.07 \pm 0.50	8.09 \pm 1.02	3.65 \pm 0.70
SacS/ST	7.29 \pm 0.43	13.44 \pm 0.98	4.98 \pm 0.43	7.34 \pm 0.82	10.78 \pm 0.87	5.42 \pm 0.82	4.57 \pm 0.45	6.80 \pm 0.89	3.24 \pm 0.59
ST/LA	8.22 \pm 1.33	15.98 \pm 3.63	5.87 \pm 1.33	6.88 \pm 0.64	12.94 \pm 1.03	4.70 \pm 0.64	4.86 \pm 0.21	7.62 \pm 0.52	3.33 \pm 0.35
ST/SacS	6.90 \pm 2.18	12.19 \pm 4.17	4.64 \pm 2.18	7.32 \pm 1.08	13.06 \pm 1.63	5.76 \pm 1.08	3.62 \pm 0.24	5.07 \pm 0.56	2.44 \pm 0.37

TABLE V: Transferring Performance of DCRNN, WAVENET and LOCALEGN on traffic flow datasets (average \pm standard deviation across 5 experimental repeats; unit for RMSE and MAE: vehicles/hour).

Source/Target	DCRNN			WAVENET			LOCALEGN		
	RMSE	MAPE (%)	MAE	RMSE	MAPE (%)	MAE	RMSE	MAPE (%)	MAE
SF/SacF	125.59 \pm 9.02	571.77 \pm 145.49	96.82 \pm 9.02	129.38 \pm 12.20	106.95 \pm 27.87	108.96 \pm 12.20	31.88 \pm 0.87	15.26 \pm 4.81	21.57 \pm 1.34
SF/SanB	102.19 \pm 6.23	299.38 \pm 63.31	78.83 \pm 6.23	90.58 \pm 6.23	103.88 \pm 26.38	77.27 \pm 6.23	27.17 \pm 0.67	14.00 \pm 2.14	19.00 \pm 0.88
SacF/SF	84.00 \pm 5.75	659.87 \pm 154.49	61.94 \pm 5.75	90.76 \pm 4.39	85.02 \pm 8.83	78.63 \pm 4.39	25.87 \pm 1.01	21.71 \pm 2.65	18.02 \pm 1.06
SacF/SanB	95.80 \pm 6.31	331.29 \pm 40.89	74.75 \pm 6.31	87.77 \pm 5.51	90.50 \pm 10.88	75.39 \pm 5.51	27.93 \pm 1.67	13.40 \pm 0.74	19.67 \pm 1.78
SanB/SF	88.32 \pm 7.09	910.14 \pm 140.04	63.38 \pm 7.09	81.96 \pm 11.46	95.34 \pm 15.22	73.89 \pm 11.46	26.44 \pm 1.76	30.95 \pm 11.12	18.97 \pm 2.08
SanB/SacF	123.60 \pm 10.77	591.62 \pm 76.52	94.44 \pm 10.77	110.59 \pm 18.08	108.27 \pm 23.19	99.32 \pm 18.08	33.83 \pm 3.51	19.19 \pm 8.19	24.02 \pm 4.30

PolyU/25209221), and a grant from the Research Institute for Sustainable Urban Development (RISUD) at the Hong Kong Polytechnic University (Project No. P0038288). The contents of this paper reflect the views of the authors, who are responsible for the facts and the accuracy of the information presented herein.

APPENDIX

A. Model Specifications

In this section, we present details of the model specifications of LOCALEGN. There are four modules in LOCALEGN, which include Encoder, NODEGRU, GN, and the Output layer. The detailed layer information of each module is listed in Table VI.

TABLE VI: Functions in LOCALEGN.

Module	Functions
Node Encoder	DenseLayer [12,64] with ReLU
Edge Encoder	DenseLayer [1,64] with ReLU
NODEGRU	[12,64]
Updating by ϕ_E	$\bar{\mathbf{e}}_k^\tau = \phi^E(\bar{\mathbf{e}}_k^\tau, \bar{\mathbf{v}}_{\text{tail}(k)}^\tau, \bar{\mathbf{v}}_{\text{head}(k)}^\tau), \forall k, \tau$
Aggregating by $\rho^{E \rightarrow V}$	DenseLayer [256,64] with ReLU
Updating by ϕ_V	Element-wise average operator $\bar{\mathbf{v}}_i^\tau = \phi^V(\bar{\mathbf{e}}_i^\tau, \bar{\mathbf{v}}_i^\tau), \forall i, \tau$
Node Decoder	DenseLayer [64,64] with ReLU
Output layer	Concatenation operator and DenseLayer [64,1] with ReLU

Besides, we provide hyper-parameters for model setting and training process in Table VII.

B. Additional Experiments

In this section, we provide results of some additional experiments to further justify the proposed structure of LOCALEGN.

TABLE VII: Hyper-parameters in LOCALEGN.

Hyper-parameters	Values
Optimizer	Adam
Learning rate	0.001
Weight decay	0.0005
Iteration	3,000
Lookback window	12
Node hidden dimension	64
Edge hidden dimension	64
Number of GRU layer	1
Number of GN layer	1

1) *Residual Graph Network*: On top of the basic architecture of Encoder, GN, and Decoder, we also try to add residual connections to the GN module. Instead of using NODEGRU, the GN module is developed to learn the differences between the input graph and the expected output graph. The encoded data will be processed by the GN module, in which we add the residual connection to update the node attributes. The design of Residual Graph Network (RGN) model is inspired by the theory of dynamical system, in which the output at $\tau+1$ can be calculated based on the input at time τ as well as the evolution function GN. Mathematically, the residual connection can be presented in Equation 9.

$$\bar{G}_{\tau+1} = \text{GN}(\bar{G}_\tau) + \bar{G}_\tau \quad (9)$$

2) *Attention Graph Network*: We also try to replace the NODEGRU module in LOCALEGN with the SELF-ATTENTION mechanism to capture the temporal dependency of the traffic data. Different from applying GRU for each node data separately, the SELF-ATTENTION module is applied to all the node data simultaneously. The reason we compare with the SELF-ATTENTION module is that recent studies indicate its strong potential in transferability [60, 63]. The proposed Attention Graph Network (AGN) can be represented in Equation 10.

$$\bar{G}_{\tau+1} = \text{GN}(\bar{G}_\tau + \text{SELF-ATTENTION}(\bar{G}_\tau)) \quad (10)$$

where the key, query and value in SELF-ATTENTION are embedded with historical node data. The outcome vector from SELF-ATTENTION is transformed to a lower dimension vector to obtain the compressed temporal patterns, which is then combined with the original node data. The combined vector is fed into an encoder to generate the input of GN in order to further infer the spatio-temporal patterns at time $\tau + 1$.

3) *Results Comparison*: Using the same experiment settings as in section IV-C, the additional two models are examined on the three speed datasets and three flow datasets, respectively. The prediction errors of LOCALEGN, RGN and AGN are listed in Table VIII and Table IX.

TABLE VIII: Performance of LOCALEGN, RGN and AGN on traffic speed datasets.

Model	LA		
	RMSE	MAPE (%)	MAE
AGN	4.45	7.18	2.80
RGN	4.34	6.94	2.73
LOCALEGN	4.24	6.88	2.70
	SacS		
	RMSE	MAPE (%)	MAE
AGN	2.94	4.21	1.91
RGN	2.55	3.53	1.58
LOCALEGN	2.56	3.72	1.65
	ST		
	RMSE	MAPE (%)	MAE
AGN	4.13	6.14	2.73
RGN	4.09	6.06	2.77
LOCALEGN	4.00	5.96	2.65

TABLE IX: Performance of LOCALEGN, RGN and AGN on traffic flow datasets.

Model	SF		
	RMSE	MAPE (%)	MAE
AGN	25.00	40.49	17.25
RGN	25.86	34.42	18.02
LOCALEGN	25.08	23.12	17.26
	SacF		
	RMSE	MAPE (%)	MAE
AGN	30.73	15.58	20.19
RGN	30.34	12.79	19.64
LOCALEGN	30.70	10.53	20.03
	SanB		
	RMSE	MAPE (%)	MAE
AGN	34.97	22.60	26.56
RGN	28.23	19.30	19.77
LOCALEGN	26.74	14.86	18.43

For traffic speed prediction, LOCALEGN outperforms RGN and AGN on both LA and ST, but slightly under-performs RGN on SacS dataset. For traffic flow prediction, LOCALEGN outperforms RGN and AGN on all datasets regarding the MAPE, but its performance is slightly lower than RGN on SacF dataset in terms of MAE and RMSE. On SF, the differences between AGN and LOCALEGN for MAE and

RMSE are within the range of ± 0.01 and negligible, but MAPE of LOCALEGN is substantially smaller than that of AGN. Overall, LOCALEGN has the best and most stable performance among the three proposed models on both traffic speed and flow prediction tasks. The detailed implementation for all the three models is also available in the code repository.

REFERENCES

- [1] F. Li, J. Feng, H. Yan, G. Jin, D. Jin, and Y. Li, “Dynamic graph convolutional recurrent network for traffic prediction: Benchmark and solution,” 2021.
- [2] G. Meena, D. Sharma, and M. Mahrishi, “Traffic prediction for intelligent transportation system using machine learning,” in *2020 3rd International Conference on Emerging Technologies in Computer Engineering: Machine Learning and Internet of Things (ICETCE)*. IEEE, 2020, pp. 145–148.
- [3] S. Kaffash, A. T. Nguyen, and J. Zhu, “Big data algorithms and applications in intelligent transportation system: A review and bibliometric analysis,” *International Journal of Production Economics*, vol. 231, p. 107868, 2021.
- [4] Y. Ma, X. Zhu, S. Zhang, R. Yang, W. Wang, and D. Manocha, “Trafficpredict: Trajectory prediction for heterogeneous traffic-agents,” in *Proceedings of the AAAI Conference on Artificial Intelligence*, vol. 33, no. 01, 2019, pp. 6120–6127.
- [5] X. Zang, H. Yao, G. Zheng, N. Xu, K. Xu, and Z. Li, “Metalight: Value-based meta-reinforcement learning for traffic signal control,” in *Proceedings of the AAAI Conference on Artificial Intelligence*, vol. 34, no. 01, 2020, pp. 1153–1160.
- [6] J. Zhou, G. Cui, S. Hu, Z. Zhang, C. Yang, Z. Liu, L. Wang, C. Li, and M. Sun, “Graph neural networks: A review of methods and applications,” *AI Open*, vol. 1, pp. 57–81, 2020.
- [7] W. Jiang and J. Luo, “Graph neural network for traffic forecasting: A survey,” *arXiv e-prints*, pp. arXiv–2101, 2021.
- [8] F. Bell and S. Smyl, “Forecasting at uber: An introduction,” Sep 2018. [Online]. Available: <https://eng.uber.com/forecasting-introduction/>
- [9] X. Yin, G. Wu, J. Wei, Y. Shen, H. Qi, and B. Yin, “Deep learning on traffic prediction: Methods, analysis and future directions,” *IEEE Transactions on Intelligent Transportation Systems*, 2021.
- [10] M. Denil, B. Shakibi, L. Dinh, M. Ranzato, and N. de Freitas, “Predicting parameters in deep learning,” 2013.
- [11] F. Emmert-Streib, Z. Yang, H. Feng, S. Tripathi, and M. Dehmer, “An introductory review of deep learning for prediction models with big data,” *Frontiers in Artificial Intelligence*, vol. 3, p. 4, 2020.
- [12] P. L. Bartlett, P. M. Long, G. Lugosi, and A. Tsigler, “Benign overfitting in linear regression,” *Proceedings of the National Academy of Sciences*, vol. 117, no. 48, pp. 30 063–30 070, 2020.

[13] G. Leduc *et al.*, “Road traffic data: Collection methods and applications,” *Working Papers on Energy, Transport and Climate Change*, vol. 1, no. 55, pp. 1–55, 2008.

[14] HKGov, “Hong kong smart city blueprint,” <https://www.smartcity.gov.hk/>, 2022.

[15] TD, “Hong kong’s transport department,” <https://data.gov.hk/en/>, 2022.

[16] V. Labs, “Sustainable travel innovations by liverpool john moores university,” Jan 2022. [Online]. Available: <https://vivacitylabs.com/sustainable-travel-innovation-liverpool/>

[17] Y. Tang, A. Qu, A. H. Chow, W. H. Lam, S. Wong, and W. Ma, “Domain adversarial spatial-temporal network: A transferable framework for short-term traffic forecasting across cities,” *arXiv preprint arXiv:2202.03630*, 2022.

[18] R. Caruana, S. Lawrence, and L. Giles, “Overfitting in neural nets: Backpropagation, conjugate gradient, and early stopping,” *Advances in neural information processing systems*, pp. 402–408, 2001.

[19] A. Ghasemian, H. Hosseini-mardi, and A. Clauset, “Evaluating overfit and underfit in models of network community structure,” *IEEE Transactions on Knowledge and Data Engineering*, vol. 32, no. 9, pp. 1722–1735, 2019.

[20] P. W. Battaglia, J. B. Hamrick, V. Bapst, A. Sanchez-Gonzalez, V. Zambaldi, M. Malinowski, A. Tacchetti, D. Raposo, A. Santoro, R. Faulkner *et al.*, “Relational inductive biases, deep learning, and graph networks,” 2018.

[21] S. Seo and Y. Liu, “Differentiable physics-informed graph networks,” *arXiv preprint arXiv:1902.02950*, 2019.

[22] A. Sanchez-Gonzalez, N. Heess, J. T. Springenberg, J. Merel, M. Riedmiller, R. Hadsell, and P. Battaglia, “Graph networks as learnable physics engines for inference and control,” in *International Conference on Machine Learning*. PMLR, 2018, pp. 4470–4479.

[23] J. Gilmer, S. S. Schoenholz, P. F. Riley, O. Vinyals, and G. E. Dahl, “Neural message passing for quantum chemistry,” in *International conference on machine learning*. PMLR, 2017, pp. 1263–1272.

[24] Y. Li, R. Yu, C. Shahabi, and Y. Liu, “Diffusion convolutional recurrent neural network: Data-driven traffic forecasting,” in *International Conference on Learning Representations*, 2018.

[25] Z. Wu, S. Pan, G. Long, J. Jiang, and C. Zhang, “Graph wavenet for deep spatial-temporal graph modeling,” *arXiv preprint arXiv:1906.00121*, 2019.

[26] L. Zhao, Y. Song, C. Zhang, Y. Liu, P. Wang, T. Lin, M. Deng, and H. Li, “T-gcn: A temporal graph convolutional network for traffic prediction,” *IEEE Transactions on Intelligent Transportation Systems*, vol. 21, no. 9, pp. 3848–3858, 2020.

[27] B. Yu, H. Yin, and Z. Zhu, “Spatio-temporal graph convolutional networks: A deep learning framework for traffic forecasting,” *arXiv preprint arXiv:1709.04875*, 2017.

[28] Z. Cui, K. Henrickson, R. Ke, and Y. Wang, “Traffic graph convolutional recurrent neural network: A deep learning framework for network-scale traffic learning and forecasting,” *IEEE Transactions on Intelligent Transportation Systems*, vol. 21, no. 11, pp. 4883–4894, 2020.

[29] S. Guo, Y. Lin, N. Feng, C. Song, and H. Wan, “Attention based spatial-temporal graph convolutional networks for traffic flow forecasting,” in *Proceedings of the AAAI Conference on Artificial Intelligence*, vol. 33, no. 01, 2019, pp. 922–929.

[30] Z. Diao, X. Wang, D. Zhang, Y. Liu, K. Xie, and S. He, “Dynamic spatial-temporal graph convolutional neural networks for traffic forecasting,” in *Proceedings of the AAAI conference on artificial intelligence*, vol. 33, no. 01, 2019, pp. 890–897.

[31] F. Scarselli, M. Gori, A. C. Tsoi, M. Hagenbuchner, and G. Monfardini, “The graph neural network model,” *IEEE transactions on neural networks*, vol. 20, no. 1, pp. 61–80, 2008.

[32] G. Guo and W. Yuan, “Short-term traffic speed forecasting based on graph attention temporal convolutional networks,” *Neurocomputing*, vol. 410, pp. 387–393, 2020.

[33] Z. C. Lipton, J. Berkowitz, and C. Elkan, “A critical review of recurrent neural networks for sequence learning,” *arXiv preprint arXiv:1506.00019*, 2015.

[34] Y. Yu, X. Si, C. Hu, and J. Zhang, “A review of recurrent neural networks: Lstm cells and network architectures,” *Neural computation*, vol. 31, no. 7, pp. 1235–1270, 2019.

[35] Y. Tian and L. Pan, “Predicting short-term traffic flow by long short-term memory recurrent neural network,” in *2015 IEEE international conference on smart city/SocialCom/SustainCom (SmartCity)*. IEEE, 2015, pp. 153–158.

[36] D. Li and J. Lasenby, “Spatiotemporal attention-based graph convolution network for segment-level traffic prediction,” *IEEE Transactions on Intelligent Transportation Systems*, 2021.

[37] H. Zheng, F. Lin, X. Feng, and Y. Chen, “A hybrid deep learning model with attention-based conv-lstm networks for short-term traffic flow prediction,” *IEEE Transactions on Intelligent Transportation Systems*, vol. 22, no. 11, pp. 6910–6920, 2020.

[38] X. Shi, H. Qi, Y. Shen, G. Wu, and B. Yin, “A spatial-temporal attention approach for traffic prediction,” *IEEE Transactions on Intelligent Transportation Systems*, vol. 22, no. 8, pp. 4909–4918, 2020.

[39] B. Y. Lin, F. F. Xu, E. Q. Liao, and K. Q. Zhu, “Transfer learning for traffic speed prediction: A preliminary study,” in *Workshops at the Thirty-Second AAAI Conference on Artificial Intelligence*, 2018.

[40] C. Zhang, H. Zhang, J. Qiao, D. Yuan, and M. Zhang, “Deep transfer learning for intelligent cellular traffic prediction based on cross-domain big data,” *IEEE Journal on Selected Areas in Communications*, vol. 37, no. 6, pp. 1389–1401, 2019.

[41] Y. Ren, X. Chen, S. Wan, K. Xie, and K. Bian, “Passenger flow prediction in traffic system based on deep neural networks and transfer learning method,” in *2019 4th International Conference on Intelligent Transportation Engineering (ICITE)*, 2019, pp. 115–120.

[42] C. Finn, P. Abbeel, and S. Levine, “Model-agnostic meta-learning for fast adaptation of deep networks,” in

International Conference on Machine Learning. PMLR, 2017, pp. 1126–1135.

[43] J. Snell, K. Swersky, and R. S. Zemel, “Prototypical networks for few-shot learning,” *arXiv preprint arXiv:1703.05175*, 2017.

[44] L. Cao, R. Ji, C. Wang, and J. Li, “Towards domain adaptive vehicle detection in satellite image by supervised super-resolution transfer,” in *Proceedings of the AAAI Conference on Artificial Intelligence*, vol. 30, no. 1, 2016.

[45] C. Lin, L. Li, W. Luo, K. C. Wang, and J. Guo, “Transfer learning based traffic sign recognition using inception-v3 model,” *Periodica Polytechnica Transportation Engineering*, vol. 47, no. 3, pp. 242–250, 2019.

[46] L. Wang, X. Geng, X. Ma, F. Liu, and Q. Yang, “Cross-city transfer learning for deep spatio-temporal prediction,” in *IJCAI*, 2019.

[47] J. Atwood and D. Towsley, “Diffusion-convolutional neural networks,” *Advances in neural information processing systems*, vol. 29, 2016.

[48] W. Hamilton, Z. Ying, and J. Leskovec, “Inductive representation learning on large graphs,” *Advances in neural information processing systems*, vol. 30, 2017.

[49] P. Velickovic, G. Cucurull, A. Casanova, A. Romero, P. Lio, and Y. Bengio, “Graph attention networks,” *stat*, vol. 1050, p. 20, 2017.

[50] H. Tang, Z. Huang, J. Gu, B.-L. Lu, and H. Su, “Towards scale-invariant graph-related problem solving by iterative homogeneous gnns,” *Advances in Neural Information Processing Systems*, vol. 33, 2020.

[51] A. Sanchez-Gonzalez, J. Godwin, T. Pfaff, R. Ying, J. Leskovec, and P. Battaglia, “Learning to simulate complex physics with graph networks,” in *International Conference on Machine Learning*. PMLR, 2020, pp. 8459–8468.

[52] V. Bapst, T. Keck, A. Grabska-Barwińska, C. Donner, E. D. Cubuk, S. S. Schoenholz, A. Obika, A. W. Nelson, T. Back, D. Hassabis *et al.*, “Unveiling the predictive power of static structure in glassy systems,” *Nature Physics*, vol. 16, no. 4, pp. 448–454, 2020.

[53] T. Xie, A. France-Lanord, Y. Wang, Y. Shao-Horn, and J. C. Grossman, “Graph dynamical networks for unsupervised learning of atomic scale dynamics in materials,” *Nature communications*, vol. 10, no. 1, pp. 1–9, 2019.

[54] C. Song, Y. Lin, S. Guo, and H. Wan, “Spatial-temporal synchronous graph convolutional networks: A new framework for spatial-temporal network data forecasting,” in *Proceedings of the AAAI Conference on Artificial Intelligence*, vol. 34, no. 01, 2020, pp. 914–921.

[55] J. Bruna, W. Zaremba, A. Szlam, and Y. LeCun, “Spectral networks and deep locally connected networks on graphs,” in *2nd International Conference on Learning Representations, ICLR 2014*, 2014.

[56] S. Hochreiter and J. Schmidhuber, “Long short-term memory,” *Neural Computation*, vol. 9, no. 8, pp. 1735–1780, 1997.

[57] L. Zhao, Y. Song, C. Zhang, Y. Liu, P. Wang, T. Lin, M. Deng, and H. Li, “T-gcn: A temporal graph convolutional network for traffic prediction,” *IEEE Transactions on Intelligent Transportation Systems*, vol. 21, no. 9, pp. 3848–3858, 2019.

[58] K. Cho, B. van Merriënboer, C. Gulcehre, D. Bahdanau, F. Bougares, H. Schwenk, and Y. Bengio, “Learning phrase representations using RNN encoder–decoder for statistical machine translation,” in *Proceedings of the 2014 Conference on Empirical Methods in Natural Language Processing (EMNLP)*. Doha, Qatar: Association for Computational Linguistics, Oct. 2014, pp. 1724–1734.

[59] K. He, X. Zhang, S. Ren, and J. Sun, “Deep residual learning for image recognition,” in *Proceedings of the IEEE conference on computer vision and pattern recognition*, 2016, pp. 770–778.

[60] A. Vaswani, N. Shazeer, N. Parmar, J. Uszkoreit, L. Jones, A. N. Gomez, Ł. Kaiser, and I. Polosukhin, “Attention is all you need,” *Advances in neural information processing systems*, vol. 30, 2017.

[61] X. Geng, Y. Li, L. Wang, L. Zhang, Q. Yang, J. Ye, and Y. Liu, “Spatiotemporal multi-graph convolution network for ride-hailing demand forecasting,” in *Proceedings of the AAAI conference on artificial intelligence*, vol. 33, no. 01, 2019, pp. 3656–3663.

[62] H. Yao, F. Wu, J. Ke, X. Tang, Y. Jia, S. Lu, P. Gong, J. Ye, and Z. Li, “Deep multi-view spatial-temporal network for taxi demand prediction,” in *Proceedings of the AAAI Conference on Artificial Intelligence*, vol. 32, no. 1, 2018.

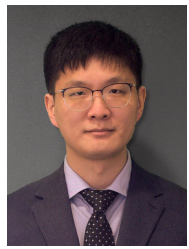
[63] J. Devlin, M.-W. Chang, K. Lee, and K. Toutanova, “Bert: Pre-training of deep bidirectional transformers for language understanding,” *arXiv preprint arXiv:1810.04805*, 2018.



Mingxi Li graduated from Sichuan University, and she is currently a Ph.D. student with the Department of Civil and Environmental Engineering at the Hong Kong Polytechnic University (PolyU). Her research interests include deep learning, multi-source traffic data mining, urban computing, and the corresponding applications in intelligent transportation systems (ITS).



Yihong Tang is a senior undergraduate student with the Department of Computer Science and Technology, School of Computer Science, Beijing University of Posts and Telecommunications (BUPT). He is now a research assistant at the Hong Kong PolyU Mobility AI Lab. His main research interests include deep learning and its applications, data mining and intelligence transportation.



Wei Ma (IEEE member) received bachelor's degrees in Civil Engineering and Mathematics from Tsinghua University, China, master degrees in Machine Learning and Civil and Environmental Engineering, and PhD degree in Civil and Environmental Engineering from Carnegie Mellon University, USA. He is currently an assistant professor with the Department of Civil and Environmental Engineering at the Hong Kong Polytechnic University (PolyU). His research focuses on intersection of machine learning, data mining, and transportation network modeling, with applications for smart and sustainable mobility systems. He has received 2020 Mao Yisheng Outstanding Dissertation Award and best paper award (theoretical track) at INFORMS Data Mining and Decision Analytics Workshop. Dr. Ma is now serving in the Early Career Editorial Advisory Board on Transportation Research Part C: Emerging Technologies.